Photocatalytic degradation of Irgalite violet dye using nickel ferrite nanoparticles

Shiljashree Vijay, Raj Mohan Balakrishnan, Eldon R. Rene and Uddandarao Priyanka

ABSTRACT

Nanotechnologies have prominent applications in the field of science and technology owing to their size-tunable properties providing a promising approach for degradation of various pollutants. In this scenario, the present work aims to study the effect of nickel ferrite nanoparticles on the degradation of Irgalite violet dye by Fenton's reaction using oxalic acid as an oxidizing agent in the presence of sunlight. The effect of pH and adsorbent dosage on the rate of dye degradation was monitored. Based on these studies it was observed that 99% dye degradation was achieved for catalyst dosage of 0.2 g, 400 ppm dye concentration and 2.0 mM oxalic acid at pH 3.0 within 60 min. The studies reveal that the degradation follows pseudo-first-order kinetics and the catalyst reusability remained constant almost for five cycles. Further, nickel ferrite nanoparticles are proven to be an efficient alternative for the removal of dyes from coloured solutions.

Key words | fenton reaction, Irgalite violet dye, nickel ferrite, oxalic acid, photocatalytic degradation

Shiljashree Vijay
Raj Mohan Balakrishnan (corresponding author)
Uddandarao Priyanka
Department of Chemical Engineering,
National Institute of Technology Karnataka,
Surathkal
575025,
India
E-mail: *rajmohanbala@gmail.com*

Eldon R. Rene
UNESCO-IHE Institute for water Education,
Westvest 7, 2601 DA Delft,
The Netherlands

INTRODUCTION

Water is a fundamental and valuable source for all forms of life on Earth. This vital source is being contaminated due to urbanization and industrialization where effluents are let into water bodies without proper treatment. Large quantities of wastewaters with high colour intensity, high chemical oxygen demand and fluctuating pH are being discharged into water bodies causing serious environmental issues affecting flora and fauna. Dyes have a complex aromatic structure and are resistant towards chemicals, heat and light, while their biodegradation is a significantly slow process. From a toxicological as well as from an ecological point of view it is essential to treat effluents containing these dyes. These diverse pollutants when allowed into the soil by migration and transformation modes cause huge global environmental issues.

Most of the conventional methods are ineffective due to the large degree of aromatics/phenols present in dye molecules. Further, they call for high operational and maintenance costs, and therefore concerns lie with the treatment of effluents by economically viable methodologies (Ye *et al.* 2017a, 2017b, 2019a, 2019b). Various physico-chemical methods like coagulation, flocculation, ion exchange, membrane separation, oxidation, nanofiltration, adsorption, catalytic ozonation (El *et al.* 2019) etc. are available for the treatment of dyes. However, some of the major limitations, such as the removal of adsorbents or the concentrated sludge produced post-remediation, are the major drawbacks of these methods. One of the alternatives to the traditional methods are the advanced oxidation processes (AOPs) which have been used to remove contaminants from drinking water and effluents. AOPs include photolysis, heterogeneous photocatalysis, electro-Fenton and photo-Fenton. Fenton is considered as an AOP that combines ferrous ions and hydrogen peroxide and other hydroxyl generating acids to promote the generation of the hydroxyl radicals in aqueous solution (Khosravi &

doi: 10.2166/aqua.2019.039

Eftekhar 2013; Lassoued *et al.* 2018). The photo-Fenton process is a typically enhanced Fenton reaction with a higher rate and faster mineralization of recalcitrant organics than the dark reaction process and can take advantage of utilizing UV irradiation from solar light. According to the light sensitivity of the photo-Fenton reaction with respect to the sunlight spectrum, the utilization of a solar light is reported to be very economic and a simple alternative compared to UV lamps, especially for treatment of wastewater at full scale. In the reaction of the photo-Fenton process, Fe^{2+} ions are oxidized by oxalic acid to Fe^{3+} to generate hydroxyl radicals. The application of Fenton's reagent as an oxidant for wastewater treatment is attractive. Among the advantages of Fenton's process relative to other oxidation techniques are the simplicity of equipment and the mild operation conditions (atmospheric pressure and room temperature); mainly for these reasons, the Fenton process has been regarded as the most economical alternative (Alalm *et al.* 2015; Deng & Zhao 2015; Santos-Juanes *et al.* 2017). In order to enhance the degradation of organic pollutants, external sources of energy have been added to the Fenton process, such as light source, and this process is called photo-Fenton process (Suna *et al.* 2007; Maaz *et al.* 2009; Shihong *et al.* 2009; Youssef *et al.* 2016). The reaction of ferrous ion (Fe^{2+}) and oxalic acid ($C_2H_2O_4$) generate hydroxyl radicals where ferric ion (Fe^{3+}) regenerates Fe^{2+} by reacting with an excess of $C_2H_2O_4$ and hydroperoxides (•OOH). The photo-Fenton process enhances the production of hydroxyl radicals by photo-reduction of Fe^{3+} to Fe^{2+} and photolysis.

Recently, various nanomaterials have been used as nanocatalysts for various applications such as sensing, detection, degradation and electrical applications (Qin *et al.* 2017; Yi *et al.* 2018a, 2018b, 2018c, 2019; Ahmadi *et al.* 2019; Baghban *et al.* 2019; Ramezanizadeh *et al.* 2019; Wang *et al.* 2019; Yang *et al.* 2019). ZnO, gold and TiO_2 are the other nanoparticles which are often reported, however, the use of magnetic $NiFe_2O_4$ nanoparticles for the photo-Fenton degradation of organic model pollutants in the presence of oxalic acid is studied. It is well known that the magnetic and electrical properties of MFe_2O_4 nanoparticles can be varied by changing the identity of the divalent M_{2+} cation or by partial substitution, while maintaining the basic crystal structure. For magnetic nanodevices and biomedical applications, MFe_2O_4 ferrites of size-tuned ferrite particles of superparamagnetic threshold were used at room temperature (Li *et al.* 2015; Weng & Huang 2015; Yahya *et al.* 2016; Behin *et al.* 2017; Shi *et al.* 2017; Sohrabi *et al.* 2017).

In this scenario, the ferrite materials based on nickel and cobalt are the subject of extensive research due to important magnetic properties like good remnant magnetization, high coercivity, magnetic anisotropy and moderate saturation magnetization. They also exhibit high electrical resistivity, and good thermal and chemical stability (Sivakumar *et al.* 2011; Sagadevan *et al.* 2018). Nickel ferrite ($NiFe_2O_4$) has an inverse spinel structure with crystal structure as AB_2O_4, in which tetrahedral sites (A) are occupied by Fe^{3+}, octahedral sites (B) by Fe^{3+} and Ni^{2+} ions formed by cubic close packing of oxygen. However, due to random distribution of divalent ions in tetrahedral and octahedral sites reverse cationic distribution in nanocrystalline spinel takes place. For instance, utilizing mesoporous $ZnFe_2O_4$-H_2O_2 under visible light for photocatalytic degradation of orange II, enhanced degradation was observed within 2 h. $NiFe_2O_4$ nanoparticles were used for the degradation of rhodamine B under visible light/oxalic system (Liu *et al.* 2012) and it was observed that they were highly stable even after seven cycles. Similarly, Fenton-like performance was also observed by which the nZVI/H_2O_2 system yielded 91.95% removal efficiency of magenta flexographic dye (Kecić *et al.* 2018). Sodium hypochlorite, hydrogen peroxide (H_2O_2) and ozone (O_3) are the other oxidizing agents used. Fenton treatment with the addition of oxalic acid has high reaction rates with ·OH and can also act as a scavenging agent in the reaction process. Due to the above-mentioned advantages, this study aims to determine the effect of nickel ferrite nanoparticles and oxalic acid using the photo-Fenton process in the degradation of Irgalite violet dye.

Irgalite violet belongs to the category of azo pigments with strong colour intensity, good transparency and rheology for aqueous, solvent-based and energy-curable inks. These characteristics of the dye make it difficult for the dye industry to decolourise or degrade the dye wash water and its effluent. Considering the unsustainable water use and water pollution due to dye effluents, in this work, the combined photo-Fenton and ferrite process was used to treat persistent dyes. Nickel ferrites due to their relatively

dry and more compact physical structure than ferric hydroxide considerably reduce sludge volume in ferrite formation. Hence, nickel ferrite is considered as a heterogeneous photo-Fenton catalyst.

MATERIALS AND METHODS

Photocatalytic experimental studies

$NiFe_2O_4$ nanoparticle synthesis was carried out by co-precipitation method as mentioned in previous work (Kollarahithlu & Balakrishnan 2018). Photocatalytic degradation of Irgalite violet dye was carried out utilizing $NiFe_2O_4$ nanoparticles in the presence of sunlight between 11a.m. and 3p.m. (IST) with an average light intensity of 6.2 kWh/m^2/day, at a temperature of 28–32 °C. Prior to irradiation, the solution was magnetically stirred in the dark to attain adsorption-desorption equilibrium for 30 min between the dye and photocatalyst. The photo-Fenton degradation of the dye was performed by varying the amount of $NiFe_2O_4$ (0.05–0.20 g), oxalic acid (0.5–2 mmol), dye concentrations (200–1,000 ppm) and pH (2.0–4.0) in a 250 mL conical flask.

Degradation efficiency estimation

Aliquots of samples were withdrawn at regular intervals of time and the intensity was measured at 547 nm using Ultraviolet–visible (UV-Vis) spectroscopy (UV-2450, Shimadzu, Japan). The photodegradation efficiency was defined as follows:

$$\text{Degradation efficiency, } \eta = \frac{C_0 - C_t}{C_0} \times 100\%$$

The pseudo-first-order kinetics is given using the following equation:

$$ln\left(\frac{C}{C_o}\right) = kt$$

where, C_0 is the initial concentration of dyes and C_t is the concentration of dye (mg L^{-1}) at certain reaction time t (min) and k is the rate constant.

RESULTS AND DISCUSSION

Effect of pH

The degradation of Irgalite violet dye by $NiFe_2O_4$ nanoparticles was studied between pH 2.0 and 4.0. At initial pH the degradation rate was minimal. The degradation efficiency was found to increase with increase in pH and attained a maximum of 99.9% degradation at pH 3.0 (Figure 1). This could be due to the increase in ferric/oxalate species and similar findings were reported by Liu *et al.* (2012), where the degradation of rhodamine B in the presence of oxalic acid was more effective at pH 3.0 confirming that the conducted Fenton oxidation process is optimum at pH 3.0 (Suna *et al.* 2007). Above pH 4.0 the degradation rate slows down to 78%; the probable reason might be due to the lower concentration of H_2O_2 production by the oxalic acid (Monteagudo *et al.* 2008). The acid environment is beneficial for the Fenton-like process, the working pH for the reaction is confined to 1.0–5.0 and the highest efficiency of the Fenton reaction occurs at pH 3.0. At pH higher than 4.0, the Fenton reaction appears to terminate due to the precipitation of Fe^{3+}. The amount of iron ions decreases because Fe^{3+} precipitates after use due to its extremely low solubility product constant even at the pH 4.0. The degradation rate increases as the pH decreases and reaches an optimum at initial pH 3.0. At the initial pH

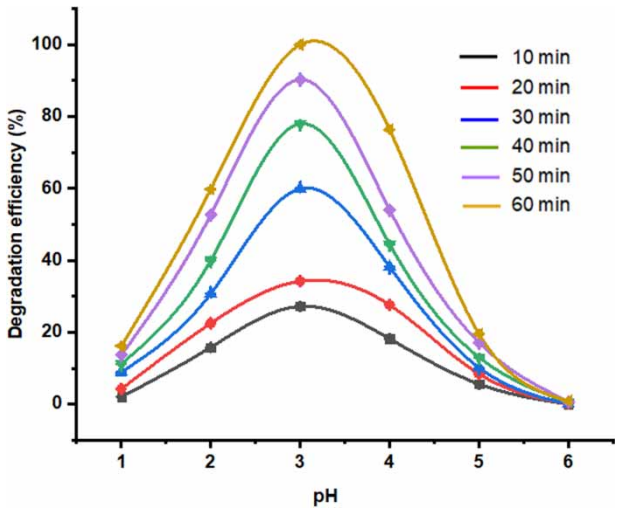

Figure 1 | Effect of pH for catalyst concentration of 0.15 g and initial dye concentration of 400 ppm.

of 2.0, a colourless solution is observed at 40 min; at pH 3.0, 99.9% of the dye is converted at 60 min reaction time and at pH 4.0 it is 78%. The oxidation potential of ˙OH is lower at pH 4.0 than that at pH 3.0. At pH > 3, the formation of hydroxyl radicals slows down because of hydrolysis of Fe^{3+} and Fe^{3+} precipitation as Fe $(OH)_3$ from the solution. Thus, the efficiency of Fenton oxidation decreases at pH higher than 3. Also, ferric hydroxide formation could decompose oxalic acid into O_2 or H_2O and, consequently, the oxidation rate is decreased as a result of the low concentration of hydroxyl radicals. Similar performance in the oxidation of dye solutions using iron-alumina catalyst in the heterogeneous Fenton process was reported where a detrimental effect on decolouration at pH > 3 was found (Barrera-Salgado *et al.* 2016; Zhou *et al.* 2016; Yi *et al.* 2018a, 2018b, 2018c).

Effect of oxalic acid concentration

The effect of initial concentration of the oxidizing agent oxalic acid was studied to determine the rate of degradation from 1.0 to 3.0 mM for the experimental condition of 0.15 g of catalyst loading at dye concentration 400 ppm and pH 3.0 for 60 min. It can be observed that the degradation rate increased with the increase in oxalic acid concentration up to 2 mM (99.5%), reached a plateau, and decreased at 2 mM by 1% for various dye concentrations (Figure 2). As

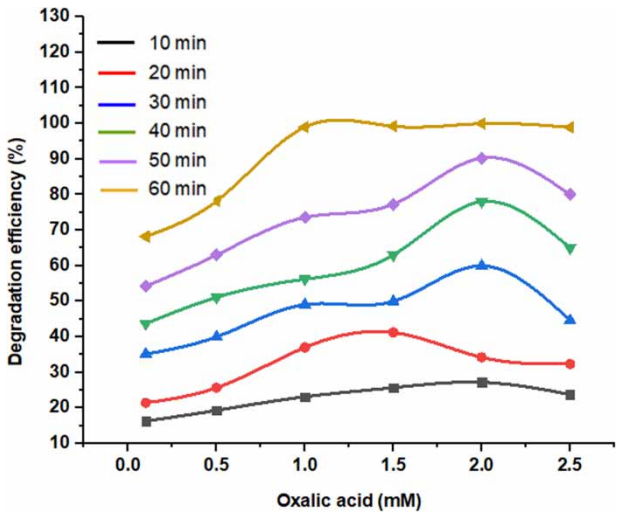

Figure 2 | Effect of oxalic concentration (1 mM, 2 mM and 3 mM) for the catalyst loading of 0.15 g for 400 ppm dye concentration at pH 3.0.

the dye concentration increased, the degradation efficiency decreased; this is because at higher concentrations of dye the number of active sites decreases, which is due to absorption of more dye molecules on the catalyst surface. This could be attributed to the hindering effect of the dye molecules on the production of •OH radicals and H_2O_2 leading to reduction in the rate of degradation. A concentration of 1.0 mM of magnetic $NiFe_2O_4$ and oxalic acid increased to 2 mM concentration leads to a high degradation rate under irradiation, indicating that $NiFe_2O_4$ is a heterogeneous Fenton catalyst. The degradation rate increases with increased oxalic concentration from 0.1 mM to 2.5 mM and then reaches a plateau at concentrations greater than 1.0 mM. This phenomenon can be attributed to forming of the predominant species $[FeIII(C_2O_4)n]^{3-2n}$ on the solid catalyst surface; its concentration reaches a maximum when the concentration of oxalic acid is 2.0 mM in solution. The reason for the optimum degradation at 2 mM of oxalic acid could be due to the generation of more OH radicals and Fe^{2+} ions (Liu *et al.* 2012) With the addition of oxalic acid, the degradation ratio of the dye is only 3.9% without irradiation. A 5% increase in decolourisation ratio is observed in the solution of oxalic acid and Irgalite violet without $NiFe_2O_4$ under irradiation. However, 99.99% degradation was achieved in the presence of the magnetic catalyst $NiFe_2O_4$ with the addition of 2 mM of oxalic acid crystals to the solution. The major role of oxalic acid is to enhance the oxidation process, and the reason for decreases at 2 mM may be because the excess production of OH radicals might compete among themselves and inhibit the efficiency of the degradation process.

Effect of catalyst loading

Figure 3 shows the dependence of Irgalite violet dye 400 ppm degradation on the loading of the $NiFe_2O_4$ catalyst in the presence of oxalic acid with an initial concentration of 2.0 mM. The degradation ratio at 20 min is 68.4%, 75.0%, 78.2%, 79.3% and 81.5% when the dosage of the $NiFe_2O_4$ catalyst is 0.05 g, 0.10 g, 0.15 g, 0.20 g and 0.25 g, respectively. When the concentration of the catalyst is further increased a decrease in degradation efficiency is observed. At the initial stage, the increase of the dosage of the catalyst leads to an obvious rise of the degradation

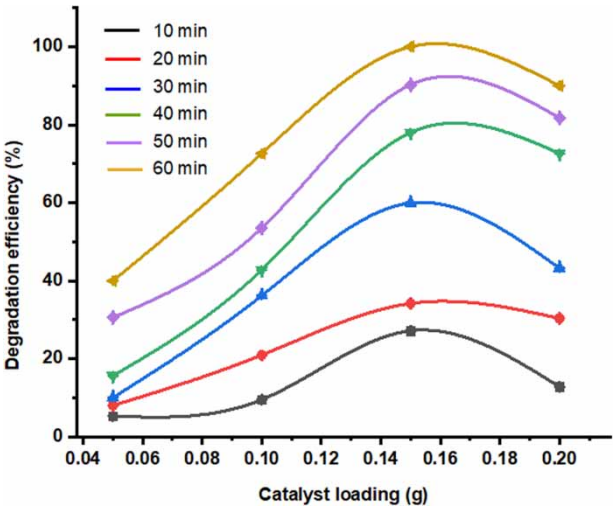

Figure 3 | Effect of time for catalyst dosage (0.05 g, 0.1 g, 0.15 g and 2.0 g) for 400 ppm of the dye concentration and 2 mM of oxalic acid maintained at pH 3.0.

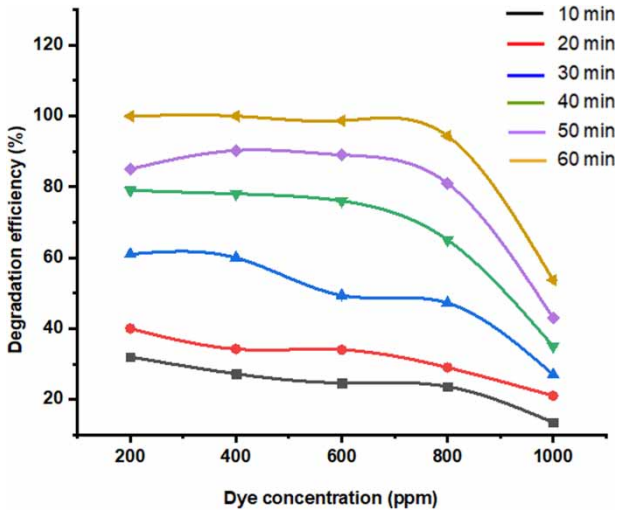

Figure 4 | Effect of dye concentration at 0.15 g catalyst loading and 2 mM of oxalic acid maintained at pH 3.0.

ratio. However, the dosage of nickel ferrite from 0.20 g to 0.25 g only results in a small change of 2% and this difference almost disappears at 30 min. The observed trend is explained on the basis that on increasing the Fe^{2+} ions in the reaction mixture, there is an enhanced generation of •OH radicals, consequently increasing the rate of photodegradation (Kakodia *et al.* 2013). After the addition of optimum Fe^{2+} ions, the higher dose of Fe^{2+} results in a brown turbidity that causes the recombination of •OH radicals and Fe^{2+} reacts with •OH as a scavenger. Therefore, on further increase, the rate decreases. Hence, 0.15 g $NiFe_2O_4$ was used in our experiments.

Effect of dye concentration

The concentrations ranging from 200 ppm to 1,000 ppm were taken individually and degradation studies carried out. The maximum degradation percentage observed for Irgalite violet is 99.995% for 400 ppm within 60 min at pH 3.0, as shown in Figure 4. There is a gradual decrease in the percentage of degradation as concentration of the dye concentration increases due to the occupancy of active sites on the catalyst by the dye molecules (Ameta *et al.* 2012). Since the amount of hydroxyl radicals generated by the given concentration of photocatalyst has been scavenged by the increase of dye molecules, a decrease in degradation efficiency is observed.

Effect of contact time

It was observed that the degradation efficiency of nickel ferrite magnetic nanoparticles over Irgalite violet dye effluent was greater in the presence of solar radiation compared to the absence of solar light, as shown in Figure 5. In the presence of light source, the photons excite the surface electrons of the catalyst, whereby these electrons move from the valence band to the conduction band leaving positive holes in the valence band, which further reacts with water

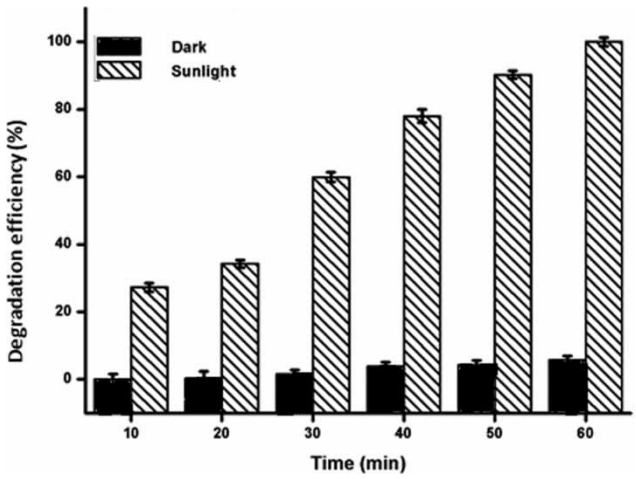

Figure 5 | Dye degradation in the presence and absence of solar light dye at 400 ppm dye concentration, 0.15 g catalyst loading and 2 mM of oxalic acid maintained at pH 3.0.

to release hydroxyl ions that degrade the dyes. Oxalic acid also contributes to the production of hydroxyl radicals which enhances the rate of degradation. As the irradiation time proceeds the degradation efficiency was found to increase. It is evident that in the presence of solar irradiation the photo catalyst (nickel ferrite) had degraded about 99.995% of Irgalite violet whereas in the absence of solar irradiation, the degradation efficiency had dropped to 29% within 60 min. In addition, the degradation rate was observed to remain almost constant after 60 min due to the competitiveness of the parent dye molecules with intermediate/short chain aliphatics during the photocatalytic degradation process (Muruganandham & Swaminathan 2006). Since the batch studies were carried out in aqueous solutions, these radicals contribute to the degradation of dye under solar irradiation in the absence of nickel ferrite nanoparticles and showed 17% degradation efficiency. This may be due to the presence of minute concentrations of hydroxyl radicals generated in water. The photons of solar light generate hydroxyl (OH) radicals due to the water molecules present in the system.

The major challenge encountered during this work is optimizing the pH, since the optimum pH is around 3.0 in the Fenton treatment which is acidic. The modified Fenton oxidation process is improved by using oxidizing agents which, in turn, increase the •OH radicals' formation to improve the efficiency of the system, and the use of $NiFe_2O_4$ nanoparticles, due to the presence of Fe^{2+}, showed strong reactivity to catalyse dyes at various conditions. The band gap of the synthesized $NiFe_2O_4$ nanoparticles for this study is 2.14 eV. Moreover, its catalytic stability can be maintained for multiple cycles and it can be a promising treatment. Even though economic feasibility was not the focus of this investigation, since this method uses solar light for the Fenton process costs, the only costs involved in the study are $NiFe_2O_4$ nanoparticles and the oxidizing agent oxalic acid. Furthermore, the use of solar energy has brought advantages since it widened the range of reactant concentrations that could be used and still achieved very satisfactory treatment performances, making it reasonable to state that the lower the number of reactants, the more economically feasible the treatment becomes (Pignatello *et al.* 2006; Hansson *et al.* 2012; Usman *et al.* 2016).

Kinetic study of photodegradation

The reaction rate constant was calculated from the slopes C/C_o against time as shown in Figure 6. The correlation constant for the fitted line was calculated to be $R^2 = 0.99$ and rate constant (k) was calculated to be 0.0223 min^{-1}. The half-life, $t_{1/2}$ of the pseudo-first-order reaction given by $t_{1/2} = 0.693/k$ was deduced to be 31.07 min.

The possible mechanism for photodegradation of Irgalite violet dye over MFe_2O_4 (M = Ni) and the active species for photodegradation of dye could be produced by three pathways. When ferrite was irradiated in the presence of solar light, the electron/hole (e^-/h^+) pair was generated on the surface:

$$MFe_2O_4 + h\upsilon \rightarrow MFe_2O_4(e^-_{CB} + h^+_{VB})$$

The photogenerated h^+_{VB} could react with water or hydroxyl ion (H_2O or OH^-) to generate hydroxyl radical:

$$h^+_{VB} + H_2O \rightarrow H^+ + OH$$

$$h^+_{VB} + OH^- \rightarrow OH^{\cdot}$$

The photogenerated electron e^-_{CB} could be captured by $C_2H_2O_4$ to yield OH; limiting the recombination of holes and electrons thus enhances the photocatalytic activity:

$$C_2H_2O_4 + e^-_{CB} \rightarrow OH^- + OH^{\bullet} + CO_2$$

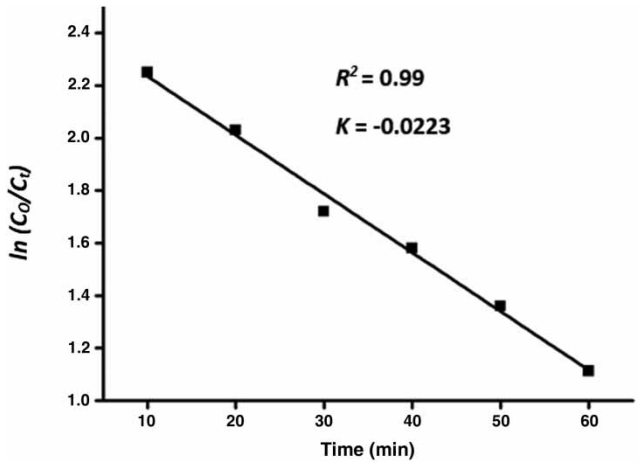

Figure 6 | Plot of pseudo-first-order kinetics of photodegradation of Irgalite violet dye mechanism for degradation of Irgalite violet dye by photo-Fenton process.

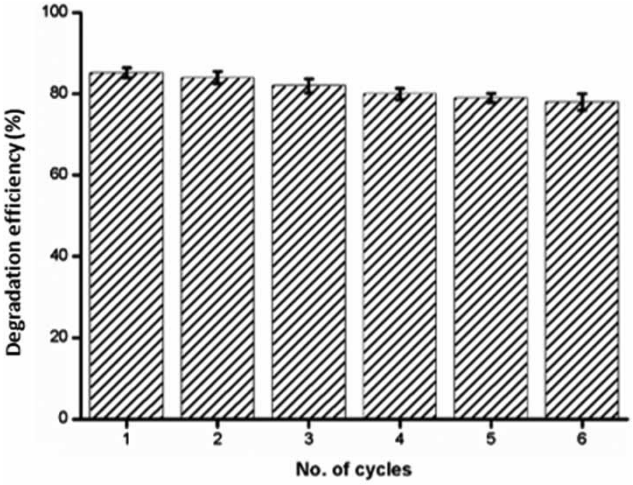

Figure 7 | Effect of catalyst reuse on Irgalite dye degradation.

The reaction of $C_2H_2O_4$ with Fe(III) on the surface of ferrite and Fe(II) generated Fenton reagent which produced hydroxyl radical:

$$Fe^{3+} + C_2H_2O_4 \rightarrow Fe^{2+} + HOO^{\bullet} + H^{+} + CO_2$$

$$Fe^{2+} + C_2H_2O_4 \rightarrow Fe^{3+} + OH^{\bullet} + OH^{-} + CO_2$$

Since OH· was produced by three pathways, enhancement in the rate of degradation was observed. The hydroxyl radical produced by the above three pathways was the main active species for degradation of Irgalite violet dye.

Recyclability of the nanoparticles

The same catalyst was washed with ethanol and distilled water and dried at 60 °C for seven times. The catalyst exhibited activity with almost the same efficiency up to six runs, as shown in Figure 7. With the reuse of catalyst the active sites of the catalyst become occupied, therefore a decrease in the efficiency is observed after six runs. The decrease in activity could be due to the loss in the activity of the catalyst during washing and drying. Figure 8(a) and 8(b) depict the morphology of nanoparticles before and after six runs.

CONCLUSION

The nickel ferrite nanoparticles synthesized by co-precipitation method were found to be stable under acidic conditions for the degradation of Irgalite dye effluent. Further, the dye was degraded completely within 60 min in the presence of 0.15 g of the nickel ferrite catalyst ($k = 0.0223\ min^{-1}$) and adding oxalic acid (2 mM) enhanced the degradation efficiency of the nanoparticles (99.95%). The UV absorbance peaks of the dye solution after the photodegradation process showed no peaks of the dye which confirms the degradation of the dye. Therefore, it can be concluded that this study can effectively be used for the degradation of dye effluents from industries. Further, this approach to dye degradation offers a simple and

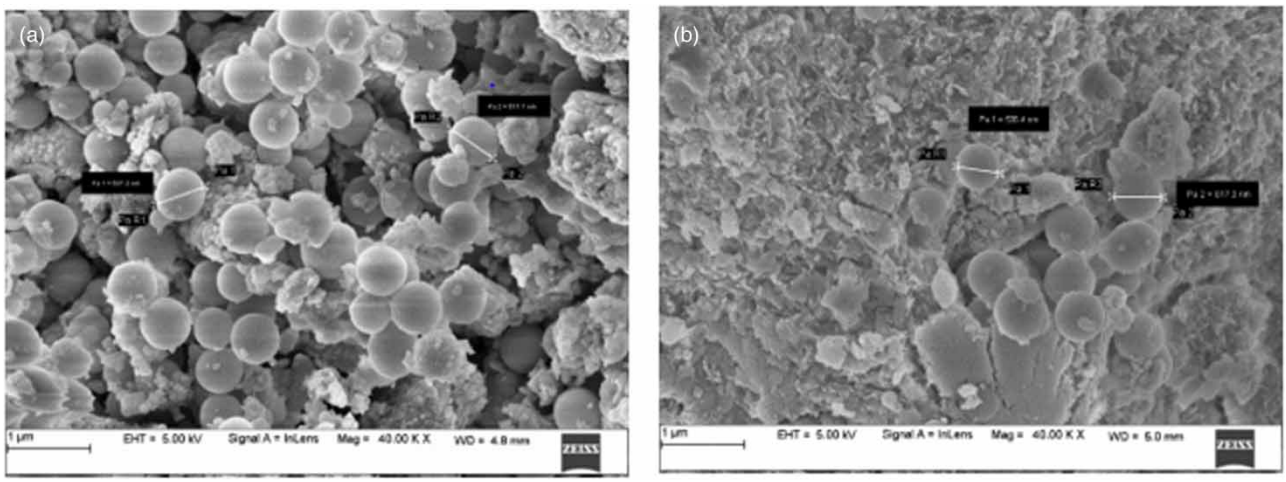

Figure 8 | SEM images of $NiFe_2O_4$ nanoparticles: (a) pure and (b) after six runs.

efficient catalyst and does not require any special conditions for the degradation process. The major limitation of this work is the pH as it is operated at acidic pH 3.0. The work can be improved by changing various heterogenous catalysts and oxidizing agents to widen the spectrum of the working pH, thereby improving the efficiency. However, the present work is a cost-effective and feasible method. Further, due to nickel ferrite's relatively dry and more compact physical structure than ferric hydroxide, ferrite formation considerably reduces sludge volume.

REFERENCES

Ahmadi, M. H., Mohseni-Gharyehsafa, B., Farzaneh-Gord, M., Jilte, R. D., Kumar, R. & Chau, K. W. 2019 Applicability of connectionist methods to predict dynamic viscosity of silver/water nanofluid by using ANN-MLP, MARS and MPR algorithms. *Engineering Applications of Computational Fluid Mechanics* **13** (1), 220–228.

Alalm, M. G., Tawfik, A. & Ookawara, S. 2015 Degradation of four pharmaceuticals by solar photo-Fenton process: kinetics and costs estimation. *Journal of Environmental Chemical Engineering* **3** (1), 46–51.

Ameta, N., Sharma, J. & Chanderia, K. 2012 Degradation of crystal violet using copper modified iron oxide as heterogeneous photo-fenton reagent. *Journal of Iranian Chemical Research* **5** (4), 241–253.

Baghban, A., Jalali, A., Shafiee, M., Ahmadi, M. H. & Chau, K. W. 2019 Developing an ANFIS-based swarm concept model for estimating the relative viscosity of nanofluids. *Engineering Applications of Computational Fluid Mechanics* **13** (1), 26–39.

Barrera-Salgado, K. E., Ramírez-Robledo, G., Álvarez-Gallegos, A., Pineda-Arellano, C. A., Sierra-Espinosa, F. Z., Hernández-Pérez, J. A. & Silva-Martínez, S. 2016 Fenton process coupled to ultrasound and UV light irradiation for the oxidation of a model pollutant. *Journal of Chemistry* **2016**, Article ID 4262530, 1–7.

Behin, J., Akbari, A., Mahmoudi, M. & Khajeh, M. 2017 Sodium hypochlorite as an alternative to hydrogen peroxide in Fenton process for industrial scale. *Water Research* **121**, 120–128.

Deng, Y. & Zhao, R. 2015 Advanced oxidation processes (AOPs) in wastewater treatment. *Current Pollution Reports* **1** (3), 167–176.

El, H. K., Kalnina, D. & Turks, M. 2019 Enhanced degradation of an azo dye by catalytic ozonation over Ni-containing layered double hydroxide nanocatalyst. *Separation and Purification Technology* **210**, 764–774.

Hansson, H., Kaczala, F., Marques, M. & Hogland, W. 2012 Photo-Fenton and Fenton oxidation of recalcitrant industrial wastewater using nanoscale zero-valent iron. *International Journal of Photoenergy* **2012**, Article ID 531076, 1–11.

Kakodia, A. K., Gurjar, L., Ameta, S. C. & Sharma, B. K. 2013 Photodegradation of acid violet 90 in aqueous solution by photo-Fenton reagent. *International Journal of Chemical Sciences* **11**, 855–864.

Kecić, V., Đurđa, K., Miljana, P., Ognjan, L., Milena, B. T., Dragana, T. P. & Božo, D. 2018 Optimization of azo printing dye removal with oak leaves-nZVI/H_2O_2 system using statistically designed experiment. *Journal of Cleaner Production* **202**, 65–80.

Khosravi, I. & Eftekhar, M. 2013 Characterization and evaluation catalytic efficiency of $NiFe_2O_4$ nano spinel in removal of reactive dye from aqueous solution. *Powder Technology* **250**, 147–153.

Kollarahithlu, S. C. & Balakrishnan, R. M. 2018 Adsorption of ibuprofen using cysteine-modified silane-coated magnetic nanomaterial. *Environmental Science and Pollution Research International* 1–10.

Lassoued, A., Mohamed, S. L., Santiago, G. G., Brahim, D., Salah, A. & Abdellatif, G. 2018 Synthesis and characterization of Ni-doped α-Fe_2O_3 nanoparticles through co-precipitation method with enhanced photocatalytic activities. *Journal of Materials Science: Materials in Electronics* **29** (7), 5726–5737.

Li, Y., Li, F., Li, F., Yuan, F. & Wei, P. 2015 Effect of the ultrasound–Fenton oxidation process with the addition of a chelating agent on the removal of petroleum-based contaminants from soil. *Environmental Science and Pollution Research* **22** (23), 18446–18455.

Liu, S. Q., Feng, L. R., Nan, X., Chen, Z. G. & Wang, X. M. 2012 Magnetic nickel ferrite as a heterogeneous photo-Fenton catalyst for the degradation of rhodamine B in the presence of oxalic acid. *Chemical Engineering Journal* **203**, 432–439.

Maaz, K., Karim, S., Mumtaz, A., Hasanain, S. K., Liu, J. & Duan, J. L. 2009 Synthesis and magnetic characterization of nickel ferrite nanoparticles prepared by co-precipitation route. *Journal of Magnetism and Magnetic Materials* **321** (12), 1838–1842.

Monteagudo, J. M., Durán, A. & López, A. C. 2008 Homogeneus ferrioxalate-assisted solar photo-Fenton degradation of Orange II aqueous solutions. *Applied Catalysis B Environmental* **83** (1–2), 46–55.

Muruganandham, M. & Swaminathan, M. 2006 Photocatalytic decolourisation and degradation of Reactive Orange 4 by TiO_2-UV process. *Dyes and Pigments* **68** (2–3), 133–142.

Pignatello, J. J., Oliveros, E. & MacKay, A. 2006 Advanced oxidation processes for organic contaminant destruction based on the Fenton reaction and related chemistry. *Critical Reviews in Environmental Science and Technology* **36** (1), 1–84.

Qin, L., Zeng, G., Lai, C., Huang, D., Zhang, C., Xu, P., Hu, T., Liu, X., Cheng, M., Liu, Y. & Hu, L. 2017 A visual application of gold nanoparticles: simple, reliable and sensitive detection of kanamycin based on hydrogen-bonding recognition. *Sensors and Actuators B: Chemical* **243**, 946–954.

Ramezanizadeh, M., Alhuyi Nazari, M., Ahmadi, M. H. & Chau, K. W. 2019 Experimental and numerical analysis of a nanofluidic thermosyphon heat exchanger. *Engineering Applications of Computational Fluid Mechanics* **13** (1), 40–47.

Sagadevan, S., Chowdhury, Z. Z. & Rafique, R. F. 2018 Preparation and characterization of nickel ferrite nanoparticles via co-precipitation method. *Materials Research* **21**, 1–5.

Santos-Juanes, L., Einschlag, F. G., Amat, A. M. & Arques, A. 2017 Combining ZVI reduction with photo-Fenton process for the removal of persistent pollutants. *Chemical Engineering Journal* **310**, 484–490.

Shi, J., Long, T., Ying, R., Wang, L., Zhu, X. & Lin, Y. 2017 Chemical oxidation of bis (2-chloroethyl) ether in the Fenton process: kinetics, pathways and toxicity assessment. *Chemosphere* **180**, 117–124.

Shihong, X., Daolun, F. & Wenfeng, S. 2009 Preparations and photocatalytic properties of visible-light-active zinc ferrite-doped TiO_2 photocatalyst. *Journal of Physical Chemistry C* **113** (6), 2463–2467.

Sivakumar, P., Ramesh, R., Ramanand, A., Ponnusamy, S. & Muthamizhchelvan, C. 2011 Synthesis and characterization of nickel ferrite magnetic nanoparticles. *Materials Research Bulletin* **46** (12), 2208–2211.

Sohrabi, M. R., Khavaran, A., Shariati, S. & Shariati, S. 2017 Removal of Carmoisine edible dye by Fenton and photo Fenton processes using Taguchi orthogonal array design. *Arabian Journal of Chemistry* **10**, S3523–S3531.

Suna, J. H., Sun, S. P., Fan, M. H., Guo, H. Q., Qiao, L. P. & Sun, R. X. 2007 A kinetic study on the degradation of p-nitroaniline by Fenton oxidation process. *Journal of Hazardous Materials* **148** (1–2), 172–177.

Usman, M., Hanna, K. & Haderlein, S. 2016 Fenton oxidation to remediate PAHs in contaminated soils: a critical review of major limitations and counter-strategies. *Science of the Total Environment* **569**, 179–190.

Wang, H., Zeng, Z., Xu, P., Li, L., Zeng, G., Xiao, R., Tang, Z., Huang, D., Tang, L., Lai, C. & Jiang, D. 2019 Recent progress in covalent organic framework thin films: fabrications, applications and perspectives. *Chemical Society Reviews* **48** (2), 488–516.

Weng, C. H. & Huang, V. 2015 Application of Fe^0 aggregate in ultrasound enhanced advanced Fenton process for decolorization of methylene blue. *Journal of Industrial and Engineering Chemistry* **28**, 153–160.

Yahya, M. S., El Karbane, M., Oturan, N., El Kacemi, K. & Oturan, M. A. 2016 Mineralization of the antibiotic levofloxacin in aqueous medium by electro-Fenton process: kinetics and intermediate products analysis. *Environmental Technology* **37** (10), 1276–1287.

Yang, Y., Zhang, C., Huang, D., Zeng, G., Huang, J., Lai, C., Zhou, C., Wang, W., Guo, H., Xue, W. & Deng, R. 2019 Boron nitride quantum dots decorated ultrathin porous g-C3N4: intensified exciton dissociation and charge transfer for promoting visible-light-driven molecular oxygen activation. *Applied Catalysis B: Environmental* **245**, 87–99.

Ye, S., Zeng, G., Wu, H., Zhang, C., Liang, J., Dai, J., Liu, Z., Xiong, W., Wan, J., Xu, P. & Cheng, M. 2017a Co-occurrence and interactions of pollutants, and their impacts on soil remediation – A review. *Critical Reviews in Environmental Science and Technology* **47** (16), 1528–1553.

Ye, S., Zeng, G., Wu, H., Zhang, C., Dai, J., Liang, J., Yu, J., Ren, X., Yi, H., Cheng, M. & Zhang, C. 2017b Biological technologies for the remediation of co-contaminated soil. *Critical Reviews in Biotechnology* **37** (8), 1062–1076.

Ye, S., Yan, M., Tan, X., Liang, J., Zeng, G., Wu, H., Song, B., Zhou, C., Yang, Y. & Wang, H. 2019a Facile assembled biochar-based nanocomposite with improved graphitization for efficient photocatalytic activity driven by visible light. *Applied Catalysis B: Environmental* **250**, 78–88.

Ye, S., Zeng, G., Wu, H., Liang, J., Zhang, C., Dai, J., Xiong, W., Song, B., Wu, S. & Yu, J. 2019b The effects of activated biochar addition on remediation efficiency of co-composting with contaminated wetland soil. *Resources, Conservation and Recycling* **140**, 278–285.

Yi, H., Jiang, M., Huang, D., Zeng, G., Lai, C., Qin, L., Zhou, C., Li, B., Liu, X., Cheng, M. & Xue, W. 2018a Advanced photocatalytic Fenton-like process over biomimetic hemin-Bi_2WO_6 with enhanced pH. *Journal of the Taiwan Institute of Chemical Engineers* **93**, 184–192.

Yi, H., Huang, D., Zeng, G., Lai, C., Qin, L., Cheng, M., Ye, S., Song, B., Ren, X. & Guo, X. 2018b Selective prepared carbon nanomaterials for advanced photocatalytic application in environmental pollutant treatment and hydrogen production. *Applied Catalysis B: Environmental* **239**, 408–424.

Yi, H., Qin, L., Huang, D., Zeng, G., Lai, C., Liu, X., Li, B., Wang, H., Zhou, C., Huang, F. & Liu, S. 2018c Nano-structured bismuth tungstate with controlled morphology: fabrication, modification, environmental application and mechanism insight. *Chemical Engineering Journal* **358**, 480–486.

Yi, H., Yan, M., Huang, D., Zeng, G., Lai, C., Li, M., Huo, X., Qin, L., Liu, S., Liu, X. & Li, B. 2019 Synergistic effect of artificial enzyme and 2D nano-structured Bi_2WO_6 for eco-friendly and efficient biomimetic photocatalysis. *Applied Catalysis B: Environmental* **250**, 52–62.

Youssef, N. A., Shaban, S. A., Ibrahim, F. A. & Mahmoud, A. S. 2016 Degradation of methyl orange using Fenton catalytic reaction. *Egyptian Journal of Petroleum* **25** (3), 317–321.

Zhou, L., Wang, L., Zhang, J., Lei, J. & Liu, Y. 2016 Well-dispersed Fe_2O_3 nanoparticles on g-C_3N_4 for efficient and stable photo-Fenton photocatalysis under visible-light irradiation. *European Journal of Inorganic Chemistry* **2016** (34), 5387–5392.

First received 25 March 2019; accepted in revised form 28 May 2019. Available online 15 July 2019